small
NANO MICRO

Field Emission Characteristics of Contact Printed Graphene Fins

*Toby Hallam, Matthew T. Cole, William I. Milne, and Georg S. Duesberg**

Carbon nanostructures have been much sought after for cold-cathode field emission applications. Herein a printing technique is reported to controllably nanostructure chemical vapor deposited graphene into vertically standing fins. The method allows for the creation of regular arrays of bilayer graphene fins, with sharp ridges that, when printed onto gold electrodes, afford a new type of field emission electron source geometry. The approach affords tunable morphologies and excellent long term and cyclic stabilities.

1. Introduction

There has been a significant interest in field emission (FE) devices for flat panel displays, parallel electron beam lithography systems, X-ray sources, and microwave amplifiers.[1–3] Towards this end the use of nano-carbon materials as electron sources has been investigated with great intensity.[4,5] Carbon nanotubes have perhaps been the most intensely studied carbon allotrope for field emission applications due to their high aspect ratio, high resistance to electromigration, high current density carrying capabilities, low sputter coefficient, and low heat generation during emission.[6,7] Though accurate placement control has been demonstrated by electron beam lithography, large-area and inexpensive control over the size, density and contacts of the nanotubes has remained a challenge.[8,9] With the advent of graphene, many of the advantages that made CNTs appealing have been extended using these planar nano-graphitic materials. However, issues with the planar-nature of graphene requires the development of fabrication techniques capable of engineering structures in a controllable and repeatable manner, which are still lacking to date.

Chemical vapour deposition (CVD) is a low cost, highly scalable route toward the fabrication of nanocarbon electronic devices.[8,10] In the case of graphene; commercial systems have demonstrated wafer scale growth up to 300 mm, as well as roll-to-roll processing.[11] Typically, graphene is grown on metallic catalysts and post-processing involves the deposition of a thin 'handling' layer of poly(methyl methacrylate) (PMMA) and subsequent wet-etching of the catalyst.[12] Rather unfortunately, for FE applications, graphene deposited in this way has been shown to be extremely planar with subnanometer variations in surface topography. Though ideal for various electronic applications, the electron emission—which is dominated by emission from lattice defects and grain boundaries—from these atomically flat materials has, as a result, been comparatively poor, primarily due to substrate induced electrostatic shielding. Consequently, graphene will only form a useful electron emitter if its edges are effectively exploited, as they offer field enhancement factors (which are proportional to the graphene membranes aspect ratio) orders of magnitude greater than those available from CNT or nanowire emitters. Previous works have employed plasma enhanced chemical vapour deposition of graphene-like materials, however the synthesised graphene and the emitter geometries defined therein were less graphitic than CVD grown graphene on planar substrates.[13]

Dr. T. Hallam, Prof. G. S. Duesberg
Centre for Research on Adaptive Nanostructures and Nanodevices
Trinity College Dublin
Dublin 2, Ireland
E-mail: duesberg@tcd.ie
Dr. M. T Cole, Prof. W. I. Milne
Department of Engineering
Electrical Engineering Division
University of Cambridge
9 JJ Thomson Avenue
CB3 0FA, Cambridge, UK
Prof. W. I. Milne
Department of Information Display
Kyung Hee University
Seoul, 130701, Republic of Korea
Prof. G. S. Duesberg
School of Chemistry
Trinity College Dublin
Dublin 2, Ireland

DOI: 10.1002/smll.201300552

Though it is conceivable that these defects may well enhance the field emission performance, relative to mechanically exfoliated defect-free graphene for example, it is also true that such lattice defects function as electron scatter sites which inhibit electron transport across large area, millimetre-scale devices. Thus, vertically aligned, graphitic graphene planes—fabricated by a facile and inexpensive means—are desirable for emerging electron sources.

In this work, we use a micro-transfer contact printing technique to deposit CVD grown graphene onto Au-coated Si/SiO_2 substrates to form nanostructured field emission electron sources. Graphene is used to 'ink' an elastomeric stamp which is then used to print the graphene onto arbitrary surfaces. Relief patterning of the stamp causes the graphene to create folds which, after printing, form free-standing 'fins' which present high aspect ratio graphene edges perpendicular to the surface. We show that field emission from such printed films is comparable to emissive nano-carbon thin films created by graphene oxide, graphite and CNTs. The structures are fabricated in a fully controlled, large-area compatible process where the sharpness of the fin is self-aligned. The aspect ratio of the fins combined with deformation effects provides a field emission enhancement factor (β) of up to 400. Most importantly, our novel field emitters show surprisingly high temporal stabilities (±2.3% at 4.8 V/μm, 100 h) and extremely stable cyclic emission both of which underlie the potential of graphene fin field emission devices.

2. Results and Discussion

2.1. Printing

As graphene is grown on metallic catalysts, its transfer onto arbitrary substrates is an essential step for making any device.[11,14] Indeed, the transfer process is critical to the graphene quality. Polymer residues and cracks introduced during the process limit the electronic performance.[15] Thus, polymer assisted transfer techniques are viewed as a stepping stone toward particular device morphologies, rather than an opportunity in graphene processing. Here we report on a transfer printing process using structured polydimethylsiloxane (PDMS) stamps which facilitate the introduction of periodic fin-like structures into CVD graphene, as schematically depicted in **Figure 1**. Previously we reported three-dimensional folded graphene structures supported by a polymer scaffolds.[16] Here, the graphene folds into bilayer vertically standing fins, as shown in **Figure 2**.

For the printing process the graphene is transferred via a PMMA support layer onto a structured PDMS stamp, as shown in Figure 1a. Whilst still in the solvent bath, which is required to remove the PMMA, the graphene sits above the trenches on the stamp and is supported within the liquid. While drying, the surface tension causes the graphene to sink into the structures of the PDMS stamp Figure 1b giving a conformal-like coating. Complete drying of the stamp would require the graphene to increase in area by ≈200% to achieve absolute conformation with the stamp surface. This is well beyond the elastic strain limit for graphene (≈25%)[17,18] and

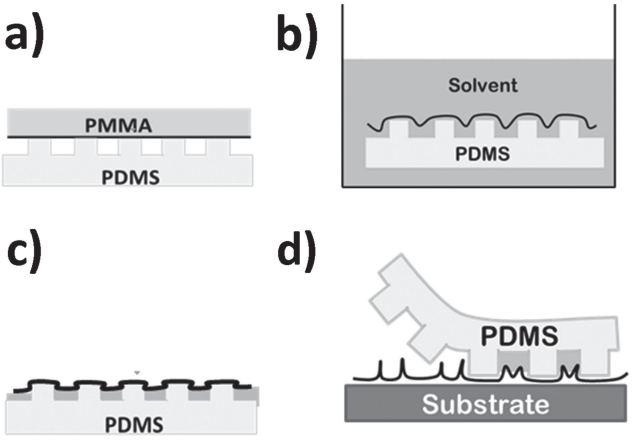

Figure 1. Schematic for 3D graphene fin printing. a) Graphene/PMMA stack transferred to structured PDMS stamp. b) Solvent bath dissolves the PMMA mediator. c) Partial drying of the stamp releases the graphene. d) Peeling of the stamp transfers the graphene to substrate defining the fin-emitter geometry.

would cause it to rupture. Instead, we print the graphene inked stamps prior to complete solvent vaporization. Surface tension effects associated with solvent removal attracts the graphene downward into the trenches of the stamp, where regions of it adhere to the trench walls, as illustrated in Figure 1c. Once the solvent was dried for 5 min, the stamp is placed upon any arbitrary substrate at which point the graphene is drawn, and adheres to the substrate (Figure 1d). The stamp is then peeled from the surface with a crack tip velocity of 5–15 μm/s leaving folds of graphene that were previously adhered to the trench walls, standing vertically on the substrate.

In this way artificial wrinkles or 'fins' are produced in graphene, as shown in the atomic force micrograph in Figure 2a. Here we show fins running perfectly parallel with a pitch of 2 μm. The fins are narrower (<25 nm) than the resolution of the experiment which is governed by the sharpness of the used AFM tip. The height of the fins varies slightly from 30–45 nm along their length (Figure 2a) and up to 120 nm in other experiments. It is believed that this variation is due to disparities in the local microscopic drying environments or possible imperfections in the graphene film. We find that the amount of film tearing varies conversely with larger fins, thereby introducing more tearing. Film transfer with a coverage of 50–90% are typical. For the FE experiments presented herein all films measured had coverage > 80% across 10 mm × 10 mm printed areas.

A scanning electron micrograph of the printed 'fins' is given in Figure 2b. The fins are well aligned with the edges of the stamp features and create a pattern of continuous fins. A small amount of meandering of the centre of the fin is visible in this image which we have measured such that the deviation of the fin from its path is ±100 nm over a distance of 30 μm. At higher resolution (not shown) the width of the fins is <4 nm, indicating that the graphene layers are conformal in a vertical bilayer configuration.

Figure 2c shows a scanning Raman map of the 2D peak full-width at half-maximum for an 8 μm × 10 μm region. We see a direct correlation between regions of wider 2D peak

small 2013,
DOI: 10.1002/smll.201300552

NANO MICRO small

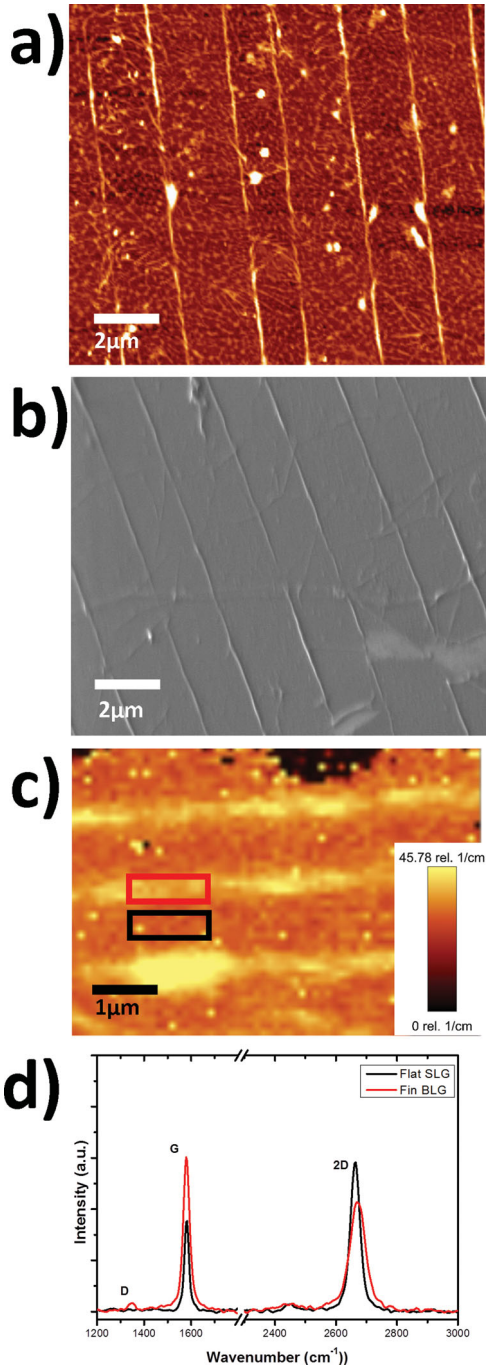

Figure 2. Graphene quality: a) AFM and b) SEM images of printed graphene fins. c) Spatially resolved Raman map of 2D peak FWHM. d) Typical Raman spectra for both fin (red) and flat (black) regions.

shape and the occurrence of the printed fins. The width of the 2D peak for graphene is known to relate to the films bilayer character due to single or multiple excitation modes available in monolayer and multilayer graphene, respectively.[19] Figure 2d is a spatially averaged Raman spectra taken from the flat monolayer graphene between the fins and the fin regions itself, as indicated on the map. Comparing the two averaged spectra, the ratio of G to 2D peak of the fin region is higher (Flat – 0.6, Fin – 1.4) the 2D peak is (Flat-39 cm^{-1}, Fin-60 cm^{-1}), and it exhibits a shoulder at 2600 cm^{-1}, all indicative of bilayer graphene. The D peak in the Raman spectra observed in the fin region can be associated with strain or defects created due to the deformation of graphene at the ridges. This confirms the bilayer nature of the fins and shows that the quality of the CVD graphene is very high as the D:G ratio is 0.04 for the flat regions.

2.2. Graphene Fin Electron Emission

The swept-field emissivity of the printed graphene fins was measured from 0–10 V/μm (**Figure 3**a). The turn-on and threshold electric fields are 1.63 V/μm and 7.23 V/μm, respectively (where the turn-on and threshold electric fields are defined as those required to extract current densities of 1 nA/cm^2[20,21] and 10 $\mu A/cm^2$, respectively). These values compare favourably with many previous reports of field emission from graphene.[13,22–24] The inset in Figure 3a shows the Fowler-Nordheim plot, for a work function of 4.5–5.0 eV.[25] Here, $\beta \approx 100$, in the pure field emission region (445) and is comparable to aspect ratio of the fins and the ab-initio electrostatic field simulations above. During the 'hot electron' emission regime the enhancement factor is significantly increased (β~ 5960) and is related to the degree of graphtization, and consequent enhanced electronic structure of the fin, rather than its topography.

To characterise the field emission properties of the printed graphene fins we have formed electrostatic simulations of the system the system (COMSOL Multiphysics (v3.4)). Here, 120 nm atomic planes of graphite protrude perpendicularly from a nominally metallic surface where the vertically-aligned pyramidal fins are separated by 2 μm, as per a typical sample. Figure 3b shows the geometry of the structure and the resulting electric field strength in areal and profile views. The models suggest $\beta \approx 50$–100, comparable with our direct measurements. Whilst the model adequately represents the structural configuration of our system, it does not however take into account the defects introduced to the graphene, such as torn edges, dangling bonds, nano-sp^3 clusters, and fold zones which are subject to extreme bond deformation. These defects are expected to improve the emissive properties of the fins and as such the modelled β values are considered lower bound estimates.

The cyclic performance of the emitter, over a course of 40 cycles, has been investigated, as shown in Figure 3c. The fins afford extremely stable cyclic performance. The standard deviation of the current across 40 cycles was consistently an order of magnitude less that the measured emission current, highlighting the reproducibility of the emission characteristics. Perhaps the most important feature of the cyclic emission data is that the turn-on voltage does not drift to higher potentials with each cycle, as is often the case for nano-carbon field emitters.[26] This negligible hysteresis, compared to typical nanocarbon field emitters,[27] may, at least in part, be due to the high degree of lattice stability during the emission and suggests that the emitter does not degrade over time and is surprisingly stable. Hysteresis is often attributed to irreversible lattice degradation via the formation of dangling bonds. Notwithstanding, it appears that the any pre-existing free C-C bonds, or those formed during

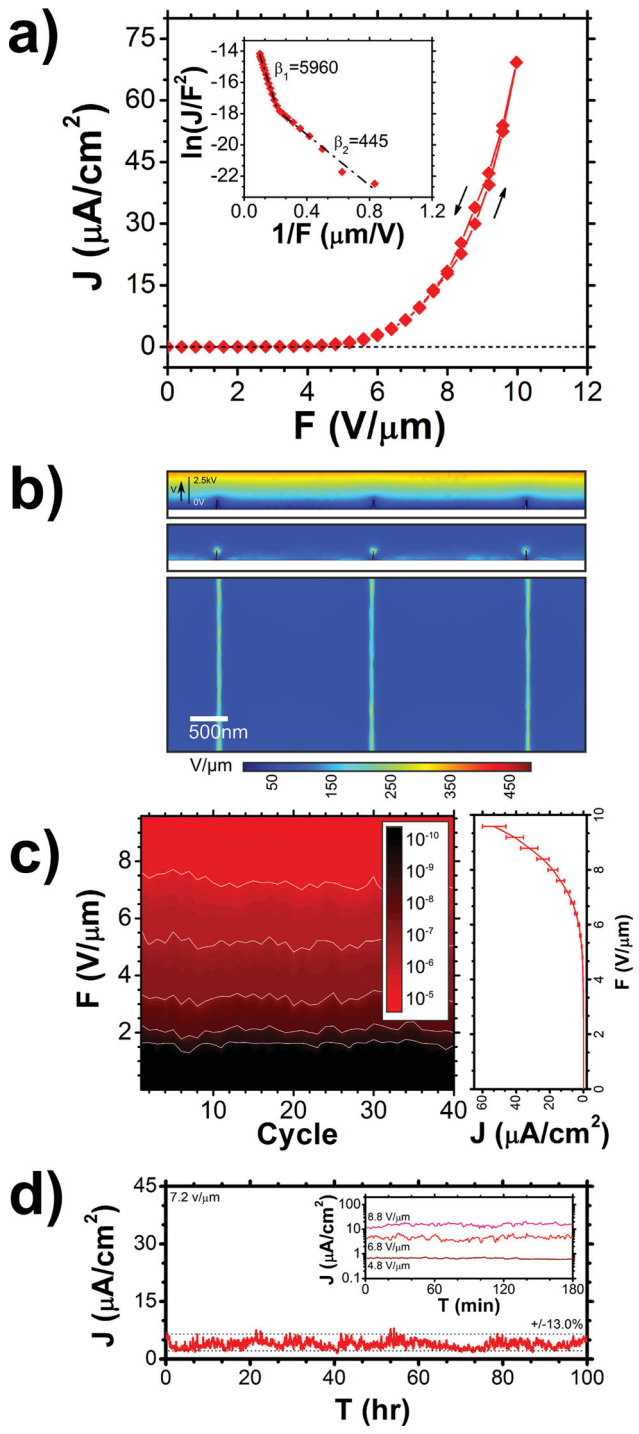

Figure 3. Field emission characteristics: a) Emission current density (J) during one complete emission sweep. Inset: Corresponding Fowler–Nordheim plot demonstrating β = 5960 (hot electron), 445 (pure FE). b) Plot of the equipotentials (0 – 2.5 kV) and the corresponding local electric field in cross-section and areal. c) Cyclic performance of the graphene fin field emitter. The intensity denotes current density, J (A/cm^2). The plot on the right shows the mean emission current over 40 cycles. d) Long-term (10 h) and short term (3 h, inset) temporal stability of the emission current over 100 h showing ±1 s.d. = 13.0% at 7.2 V/μm, and 2.3% at 4.8 V/μm.

emission, are not significant sources of structural or electronic instabilities, irrespective of their effect on the local work function, emitter topography or lattice staining.[28] The presence of surface absorbates has also been shown to inhibit hysteric emission.[29] This leads us to speculate that the graphene fins surfaces are sufficiently coated with chemisorbed species to induce the stable emission observed.

Finally, Figure 3d details an accelerated lifetime test demonstrating the emission behaviour of the fins over 100 h at 7.2 V/μm with a corresponding variation in emission current of 13.0%. Short term stability tests, conducted over 3 hours continuous operation with mean current densities of 0.65μA/cm^2(4.8V/μm),4.57μA/cm^2(6.8V/μm)and15.29μA/cm^2 (8.8 V/μm) gave a variation in emission of 2.3%, 8.9% and 6.5% respectively, confirming the surprising temporal stability of the structured graphene fin field emitters. These stabilities compare favorably to other nano-carbon-based field emission electron sources.[1,30] The higher than predicted value for the field enhancement factor combined with the stability allows us to make some tentative assertions about the emission from fin structured films. Apart from the geometric enhancement of the emission we propose that the emission originates from a distorted sp^3 crystalline geometry, principally at the ruptured graphene interfaces, or rehybridized sp^2 bonds at the fin edges—a direct consequence of bond angle deformation.[31] However, previous studies suggest that torn graphene layers are easy to mechanically relocate, and even remove from the cathode during the application of large electrostatic fields (generally > 5 V/μm).[32] This contrasts with our stability data in Figure 3c. Therefore, we suggest that the majority of field enhancement derives from the folded fin edges, which bodes well for further optimization of the fin printing technique to include higher fin densities and reduced rupturing.

3. Conclusion

In conclusion we have demonstrated an entirely new and facile approach toward the creation of free-standing vertically aligned graphene fins. The fins can be fabricated in large areas and offer precisely controllable patterns. This is the first example of CVD grown graphene fin field emitters and we have shown that these structures have a comparable turn-on voltage to other nano-carbon emitters, but show superior cyclic stability and minimal long term drift. We believe that as the structured stamping process is further refined the density of fins can be increased to meet the nearest neighbour electrostatic shielding limit, and the occurrence of tears can be reduced further to improve the performance and stability of this type of graphene, cold cathode electron source.

4. Experimental Section

Polydimethylsiloxane (PDMS) stamps were created by mixing a curing agent and PDMS prepolymer (SYLGARD 184 Silicone Elastomer Kit, Dow Corning) in a 1:5 volume ratio which were cast onto a silicon master mould fabricated by optical lithography with a standard S1813 resist process and Reactive Ion Etching using SF_6. The stamp was then cured at 22 °C at STP for 48 h. The cured stamp exhibit well-defined trenches 2 μm wide and 1.9 μm deep with a 4 μm pitch.

Graphene was prepared on 18 μm thick copper foils (99.8% Gould Electronics GmbH) using a CVD process that has been

small 2013,
DOI: 10.1002/smll.201300552

NANO MICRO small

reported in detail previously.[33] Graphene was transferred to PDMS substrates using a modified polymer-assisted method.[34] Here, 950 K PMMA was first cast onto a graphene coated foil. The copper was then etched in an ammonium persulfate (20% w/w) aqueous solution and the remaining PMMA/graphene stack rinsed in DI water before being floated onto the patterned PDMS stamp. The inked stamps were dried in a room temperature desiccator overnight.

Once transferred to the stamp the PMMA/graphene stacks were sufficiently rigid to sit flat upon the surface of the stamp (Figure 1a). We then use a 4:1 mixture of acetonitrile and ethanol to dissolve the PMMA mediator (Figure 1b). More effective solvents, such as acetone, cannot be used at they induce swelling in the PDMS and can cause the graphene to tear.[35] Once the PMMA was dissolved the graphene was then printed. Printing was carried out with a Physik Instrumente translation stage at STP. In this work we have used a Ti/Au (5 nm / 10 nm) layer on 300 nm thermal oxide on degenerately doped Si (100) substrates.

Scanning electron micrographs were acquired using a Zeiss Ultra Plus SEM. AFM images were acquired using an Asylum MFP-3D atomic force microscope. Raman spectra and mapping of the structured graphene fins were perfomed using a Witec alpha300 system equipped with a 532 nm laser excitation source. Field emission measurements were conducted in a computer-controlled, custom-built ion-pumped high vacuum chamber with a base pressure of 7×10^{-9} mbar. The system was baked for 24 h at 180 °C to remove absorbates. Electric fields were cycled from 0–2.5 kV ($\Delta V = 100$ V), with the inter-electrode cavity mechanically defined by a 250 μm alumina spacer. The emission currents were measured four times at each field and averaged accordingly.

Acknowledgements

TH and MTC contributed equally to this work. The authors thank the EU under FP7 NMP "GRAFOL" contract no. 285275 or financial support.

TH and GSD thank Science Foundation Ireland (SFI) for financial support under PICA "GREES" Contract No. PI_10/IN.1/I3030.

[1] W. Lei, C. Li, M. T. Cole, K. Qu, S. Ding, Y. Zhang, J. H. Warner, X. Zhang, B. Wang, W. I. Milne, *Carbon*, *56* 255–263 **2013**.

[2] K. B. K. Teo, E. Minoux, L. Hudanski, F. Peauger, J.-P. Schnell, L. Gangloff, P. Legagneux, D. Dieumegard, G. A. J. Amaratunga, W. I. Milne, *Nature* **2005**, *437*(7061), 968–968.

[3] K. B. K. Teo, M. Chhowalla, G. A. J. Amaratunga, W. I. Milne, P. Legagneux, G. Pirio, L. Gangloff, D. Pribat, V. Semet, V. T. Binh, W. H. Bruenger, J. Eichholz, H. Hanssen, D. Friedrich, S. B. Lee, D. G. Hasko, H. Ahmed, *J. Vac. Sci. Technol., B: Microelectron. Nanometer Struct. Process., Meas., Phenom.* **2003**, *21*(2), 693–697.

[4] R. G. Forbes, *J. Vac. Sci. Technol., B: Microelectron. Nanometer Struct. Process., Meas., Phenom.* **2010**, *28*(2), C2A43–C2A49.

[5] J. A. Driscoll, B. Cook, S. Bubin, K. Varga, *J. Appl. Phys.* **2011**, *110*(2), 024304-.

[6] M. Hamanaka, V. Mammana, P. Tatsch, *NanoCarbon* **2011**, *2013*, 1–32.

[7] D. Ye, S. Moussa, J. D. Ferguson, A. A. Baski, M. S. El-Shall, *Nano Lett.* **2012**, *12*(3), 1265–1268.

[8] G. S. Duesberg, A. P. Graham, F. Kreupl, M. Liebau, R. Seidel, E. Unger, W. Hoenlein, *Diamond Relat. Mater.* **2004**, *13*(2), 354–361.

[9] G. S. Duesberg, A. P. Graham, M. Liebau, R. Seidel, E. Unger, F. Kreupl, W. Hoenlein, *Nano Lett.* **2003**, *3*(2), 257–259.

[10] G. Aichmayr, A. Avellan, G. S. Duesberg, F. Kreupl, S. Kudelka, M. Liebau, A. Orth, A. Sanger, J. Schumann, O. Storbeck; *2007 IEEE Symposium on VLSI Technology*, **2007**, 186–187.

[11] S. Bae, H. Kim, Y. Lee, X. Xu, J.-S. Park, Y. Zheng, J. Balakrishnan, T. Lei, H. Ri Kim, Y. I. Song, Y.-J. Kim, K. S. Kim, B. Ozyilmaz, J.-H. Ahn, B. H. Hong, S. Iijima, *Nat. Nanotechnol.* **2010**, *5*(8), 574–578.

[12] Y. Ren, C. Zhu, W. Cai, H. Li, Y. Hao, Y. Wu, S. Chen, Q. Wu, R. D. Piner, R. S. Ruoff, *Nano* **2012**, *07*(01), 1150001.

[13] J. J. Wang, M. Y. Zhu, R. A. Outlaw, X. Zhao, D. M. Manos, B. C. Holloway, V. P. Mammana, *App. Phys. Lett.* **2004**, *85*(7), 1265–1267.

[14] S. Kumar, E. Rezvani, V. Nicolosi, G. S. Duesberg, *Nanotechnology* **2012**, *23*(14), 145302.

[15] N. Peltekis, S. Kumar, N. McEvoy, K. Lee, A. Weidlich, G. S. Duesberg, *Carbon* **2012**, *50*(2), 395–403.

[16] S. Winters, T. Hallam, H. Nolan, G. S. Duesberg, *Phys. Status Solidi B* **2012**, *249*(12), 2515–2518.

[17] F. Liu, P. Ming, J. Li, *Phys. Rev. B* **2007**, *76*(6), 064120.

[18] C. Lee, X. Wei, J. W. Kysar, J. Hone, *Science* **2008**, *321*(5887), 385–388.

[19] A. C. Ferrari, J. C. Meyer, V. Scardaci, C. Casiraghi, M. Lazzeri, F. Mauri, S. Piscanec, D. Jiang, K. S. Novoselov, S. Roth, A. K. Geim, *Phys. Rev. Lett.* **2006**, *97*(18), 187401.

[20] S. Hofmann, C. Ducati, B. Kleinsorge, J. Robertson, *Appl. Phys. Lett.* **2003**, *83*(22), 4661–4663.

[21] G. Pirio, P. Legagneux, D. Pribat, K. B. K. Teo, M. Chhowalla, G. A. J. Amaratunga, W. I. Milne, *Nanotechnology* **2002**, *13*(1), 1–4.

[22] C. Y. Cheng, M. Nakashima, K. Teii, *Diamond Relat. Mater.* **2012**, *27–28*(0), 40–44.

[23] X. Dong, P. Wang, W. Fang, C.-Y. Su, Y.-H. Chen, L.-J. Li, W. Huang, P. Chen, *Carbon* **2011**, *49*(11), 3672–3678.

[24] S. Santandrea, F. Giubileo, V. Grossi, S. Santucci, M. Passacantando, T. Schroeder, G. Lupina; D. A. Bartolomeo, *Appl. Phys. Lett.* **2011**, *98*(16), 163109.

[25] S. S. Datta, D. R. Strachan, E. J. Mele, A. T. C. Johnson, *Nano Lett.* **2008**, *9*(1), 7–11.

[26] M. T. Cole, K. Hou, J. H. Warner, J. S. Barnard, K. Ying, Y. Zhang, C. Li, K. B. K. Teo, W. I. Milne, *Diamond Relat. Mater.* **2012**, *23*, 66–71.

[27] Y. C. Choi, Y. M. Shin, D. J. Bae, S. C. Lim, Y. H. Lee, B. S. Lee, *Diamond Relat. Mater.* **2001**, *10*(8), 1457–1464.

[28] P. G. Collins, A. Zettl, *Phys. Rev. B* **1997**, *55*(15), 9391–9399.

[29] S. C. Lim, H. J. Jeong, Y. S. Park, D. S. Bae, Y. C. Choi, Y. M. Shin, W. S. Kim, K. H. An, Y. H. Lee, *J. Vac. Sci. Technol., A* **2001**, *19* 1786–1789.

[30] C. Li, Y. Zhang, M. T. Cole, S. G. Shivareddy, J. S. Barnard, W. Lei, B. Wang, D. Pribat, G. A. J. Amaratunga, W. I. Milne, *ACS Nano* **2012**, *6*(4), 3236–3242.

[31] Z.-S. Wu, S. Pei, W. Ren, D. Tang, L. Gao, B. Liu, F. Li, C. Liu, H.-M. Cheng, *Adv. Mater.* **2009**, *21*(17), 1756–1760.

[32] A. Y. Babenko, A. T. Dideykin, E. D. Eidelman, *Phys. Solid State* **2009**, *51*(2), 435–439.

[33] S. Kumar, N. McEvoy, H.-Y. Kim, K. Lee, N. Peltekis, E. Rezvani, H. Nolan, A. Weidlich, R. Daly, G. S. Duesberg, *Phys. Status Solidi B* **2011**, *248*(11), 2604–2608.

[34] X. Li, W. Cai, J. An, S. Kim, J. Nah, D. Yang, R. Piner, A. Velamakanni, I. Jung, E. Tutuc, S. K. Banerjee, L. Colombo, R. S. Ruoff, *Science* **2009**, *324*(5932), 1312–4.

[35] J. N. Lee, C. Park, G. M. Whitesides, *Anal. Chem* **2003**, *75*(23), 6544–6554.

Received: February 20, 2013
Revised: May 3, 2013
Published online:

small 2013,
DOI: 10.1002/smll.201300552